Journal of Applied Fluid Mechanics, Vol. 8, No. 4, pp. 911-919, 2015.
Available online at www.jafmonline.net, ISSN 1735-3572, EISSN 1735-3645.
DOI: 10.18869/acadpub.jafm.73.238.23941

Dual Solutions for MHD Jeffery–Hamel Nano-Fluid Flow in Non-parallel Walls Using Predictor Homotopy Analysis Method

N. Freidoonimehr[1†] and M. M. Rashidi[2, 3]

[1] *Young Researchers & Elite Club, Hamedan Branch, Islamic Azad University, Hamedan, Iran*
[2] *Mechanical Engineering Department, Engineering Faculty of Bu-Ali Sina University, Hamedan, Iran*
[3] *Mechanical Engineering Department, University of Michigan-Shanghai Jiao Tong University Joint Institute, Shanghai Jiao Tong University, Shanghai, Peoples Republic of China*

†*Corresponding Author Email: nfreidoonimehr@yahoo.com*

(Received July 10, 2014; accepted August 16, 2014)

ABSTRACT

The main purpose of this study is to present dual solutions for the problem of magneto-hydrodynamic Jeffery–Hamel nano-fluid flow in non-parallel walls. To do so, we employ a new analytical technique, Predictor Homotopy Analysis Method (PHAM). This effective method is capable to calculate all branches of the multiple solutions simultaneously. Moreover, comparison of the PHAM results with numerical results obtained by the shooting method coupled with a Runge-Kutta integration method illustrates the high accuracy for this technique. For the current problem, it is found that the multiple (dual) solutions exist for some values of governing parameters especially for the convergent channel cases (α = -1). The fluid in the non-parallel walls, divergent and convergent channels, is the drinking water containing different nanoparticles; Copper oxide (*CuO*), Copper (*Cu*) and Silver (*Ag*). The effects of nanoparticle volume fraction parameter (φ), Reynolds number (*Re*), magnetic parameter (*Mn*), and angle of the channel (α) as well as different types of nanoparticles on the flow characteristics are discussed.

Keywords: MHD; Nano-fluid; Jeffery–Hamel flow; Non-parallel walls; Predictor homotopy analysis method; Multiple solutions.

NOMENCLATURE

B_0	electromagnetic induction
c_i	arbitrary constant
F	self-similar velocity
f_{max}	dimensional constant
Mn	magnetic parameter
P	fluid pressure
r	radial direction in cylindrical polar coordinate
Re	Reynolds number
u	velocity component in the radial direction
x	dimensionless degree
α	semi-angle between the two inclined walls
σ	electrical conductivity
δ	prescribed parameter
H_i	auxiliary function
$\hbar$	auxiliary nonzero parameter
L	auxiliary linear operator
N	nonlinear operator
φ	nanoparticle volume fraction
θ	tangential direction in cylindrical polar coordinate
ρ	density
ν	kinematic viscosity
μ	viscosity

Subscripts

f	fluid
nf	nano-fluid
s	solid

1. INTRODUCTION

Working fluids have great demands placed upon them in terms of increasing or decreasing energy release to systems, and their influences depend on thermal conductivity, heat capacity and other physical properties in modern thermal and manufacturing processes. A low thermal conductivity is one of the most remarkable parameters that can limit the heat transfer

performance. Suspending the ultrafine solid metallic particles in technological fluids causes an increase in the thermal conductivity. This is one of the most modern and appropriate methods for increasing the coefficient of heat transfer. It is expected that the ultrafine solid particle is able to increase the thermal conductivity and heat transfer performance, since the thermal conductivity of solid metals is higher than that of base fluids. Choi and Eastman (1995) were probably the first to employ a mixture of nanoparticles and base fluid that such fluids were designated as "Nano-fluid". Experimental studies have displayed that with 1-5% volume of solid metallic or metallic oxide particles, the effective thermal conductivity of the resulting mixture can be increased by 20% compared to that of the base fluid, as stated by Eastman *et al.* (1999). Xuan and Li (2003) stated that the flow and heat transfer performance of nano-fluids under the turbulent flow in tubes.

Their experimental results showed that the convective heat transfer coefficient and Nusselt number of nano-fluids are enhanced by increasing the Reynolds number and volume fraction of nanoparticles. A wide range of review papers on nano-fluids and their different applications can be found in Bachok *et al.* (2010), Mahian *et al.* (2012), Rashidi *et al.* (2013a), Rashidi *et al.* (2014a), Sheikholeslami and Ganji (2014a).

The study of flows in converging/diverging channel is very important due to its vast engineering and industrial applications, such as enhancing heat transfer of heat exchangers for milk flowing, cold drawing operation in polymer industry, extrusion of molten polymers through converging dies, and many others, as stated by Kato and Shibanuma (1980), Hooper *et al.* (1982), Sadeghy *et al.* (2007). In recent years, this problem is extensively studied by several researchers. Moghimi *et al.* (2011) studied the MHD Jeffery–Hamel flows in non-parallel walls analytically using Homotopy analysis method (HAM). Hatami *et al.* (2014), Hatami and Ganji (2014) investigated the MHD Jeffery–Hamel nano-fluid flow in non-parallel walls using Differential Transformation Method (DTM), Least square method (LSM) and Weighted Residual Method (WRM). In another study, Moradi *et al.* (2013) discussed the nonlinear Jeffery–Hamel flow problem in a nano-fluid.

One of the most important methods for highly-nonlinear problems is the homotopy analysis method (HAM) which was firstly employed by Liao (2004a), (2004b) for the nonlinear problems, which is of fundamental interest for practical using in science and engineering. This powerful method is being employed vastly by many researchers in different practical aspects of engineering and nonlinear problems. Rashidi *et al.* (2014b) employed HAM to investigate the free convective heat and mass transfer in a steady 2D magneto-hydrodynamic fluid flow over a stretching vertical surface in porous medium. In another study, Rashidi *et al.* (2014c) investigated the MHD mixed convective heat transfer for an incompressible, laminar, and electrically conducting viscoelastic fluid flow past a permeable wedge with thermal radiation via HAM. Hayat *et al.* (2009) depicted the effects of MHD flow of an upper-convected (UCM) fluid over a stretching surface via HAM. Abbas *et al.* (2010) presented an analytical solution for the mixed convective flow in a Maxwell fluid over a stretching surface. Rashidi *et al.* (2013b) studied the first and second law analyzes of an electrically conducting fluid past a rotating disk in the presence of a uniform vertical magnetic field analytically and then applied artificial neural network and particle swarm optimization algorithm to minimize the entropy generation.

Recently, a new method related to the homotopy analysis method has been presented by Abbasbandy and Shivanian (2011), Shivanian and Abbasbandy (2014), Vosoughi *et al.* (2012), Abbasbandy and Shivanian (2014) namely Predictor Homotopy Analysis Method (PHAM). The main idea of PHAM is to rebuild the homotopy analysis method by adding rule of multiplicity of solutions and so-called prescribed parameter. This analytical technique can receive much more attention because of its accuracy and the ability to gain the solution for problems with multiplicity solutions (dual, triple, etc. solutions) (Bing-li and Yin-ping (2013)).

In this article, we check and present the dual solutions for the MHD Jeffery–Hamel nano-fluid flow in non-parallel walls via a new analytical technique, PHAM. Although the problem of Jeffery–Hamel nano-fluid in non-parallel walls are already considered in several articles by Hatami *et al.* (2014), Moradi *et al.* (2013) and Sheikholeslami *et al.* (2012) using different numerical/analytical techniques as mentioned before, dual solutions for the problem of MHD Jeffery–Hamel nano-fluid flow in non-parallel walls are firstly presented in this study. Moreover, the effects of the nanoparticle volume fraction parameter, Reynolds number, magnetic parameter, and angle of the channel as well as different types of nanoparticles; *Cuo*, *Cu* and *Ag*, on the flow velocity are discussed.

The content of this article is divided up as follows: in section 2 we derive the mathematical model that will be investigated in this study. In section 3 we implement the PHAM to solve the resulting system of nonlinear differential equations. Section 4 deals with the PHAM calculations of the multiplicity of solutions. Results are discussed in section 5. Conclusion section is also presented in section 6.

2. PROBLEM FORMULATION

Let us consider the system of cylindrical polar coordinates (r, θ, z) which steady 2D flow of an incompressible conducting viscous fluid from a source or sink at channel walls lies in planes, and intersect in z-axis. It is assumed that there are no changes with respect to z and the motion is purely in radial direction and just depends on r and θ, which means that there is no change in the flow parameter along the z direction or $\mathbf{v} = (u(r, \theta), 0)$, and moreover there is no magnetic field along

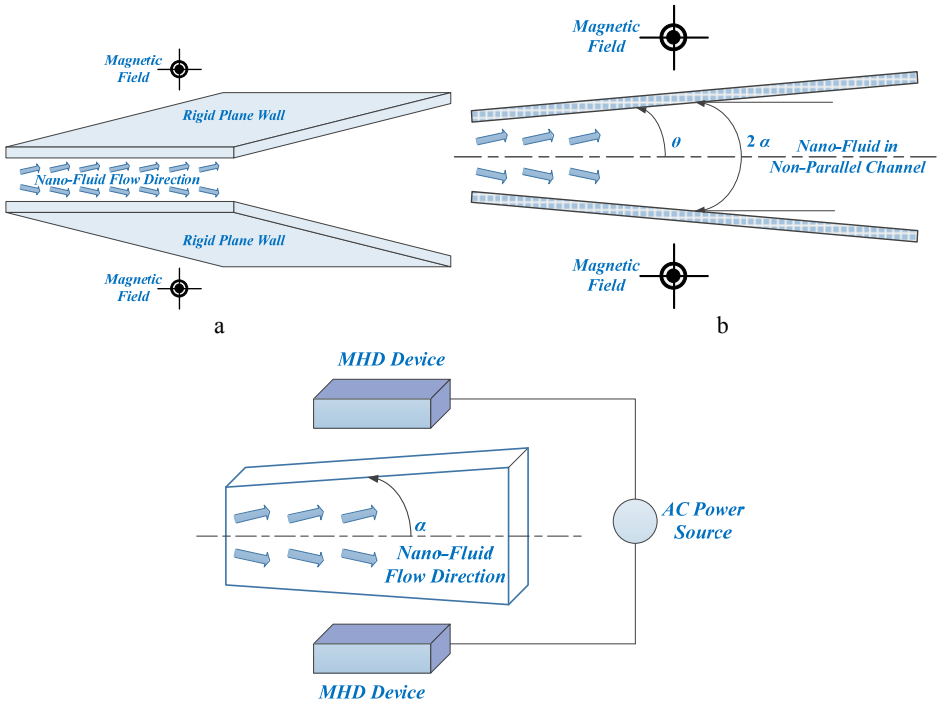

Fig. 1. Geometry of the MHD Jeffery–Hamel flow with nano-fluid in divergent channel; a) 3-D view, b) 2-D view and c) Schematic setup of problem.

z-axis. We consider that the converging/diverging channel has macro-scale and therefore no-slip condition holds at the wall. In addition, we assume that the base fluid and nanoparticles have the same velocity in an incompressible laminar flow. The coordinate system, 2D and 3D views of the problem geometry and schematic setup of problem are shown in figure 1. The equations of continuity and motion under the above considerations can be written as (Hatami and Ganji (2014), Moradi *et al.* (2013), Sheikholeslami *et al.* (2012), Sheikholeslami and Ganji (2014b)):

$$\frac{\rho_{nf}}{r}\frac{\partial\left(r\,u(r,\theta)\right)}{\partial r}\left(r\,u(r,\theta)\right)=0, \tag{1}$$

$$u(r,\theta)\frac{\partial u(r,\theta)}{\partial r}=-\frac{1}{\rho_{nf}}\frac{\partial P}{\partial r}+ \nu_{nf}\left[\frac{\partial^2 u(r,\theta)}{\partial r^2}+\frac{1}{r}\frac{\partial u(r,\theta)}{\partial r}+\frac{1}{r^2}\frac{\partial^2 u(r,\theta)}{\partial \theta^2}-\frac{u(r,\theta)}{r^2}\right]-\frac{\sigma_{nf}B_0^2}{\rho_{nf}r^2}u(r,\theta), \tag{2}$$

$$\frac{1}{\rho_{nf}r}\frac{\partial P}{\partial \theta}-\frac{2\nu_{nf}}{r^2}\frac{\partial u(r,\theta)}{\partial \theta}=0, \tag{3}$$

Subjected to the bellow boundary conditions:
At the channel centerline:

$$\frac{\partial u(r,\theta)}{\partial \theta}=0 \qquad u(r,\theta)=U_{max}$$

At the plates, making the body of the channel:

$$u(r,\theta)=0$$

where ρ_{nf} is the fluid density, P is the fluid pressure, ν_{nf} is the coefficient of kinematic viscosity, σ_{nf} is the conductivity of the fluid, and B_0 is the electromagnetic induction. In addition, μ_{nf} and ρ_{nf} are the effective dynamic viscosity and effective density of the nano-fluid, where μ_{nf} has been proposed by Brinkman (1952). The mentioned physical nano-fluid parameters are introduced as (Hatami *et al.* (2014)):

$$\rho_{nf}=(1-\varphi)\rho_f+\varphi\rho_s,$$

$$\mu_{nf}=\frac{\mu_f}{(1-\varphi)^{2.5}}, \qquad \nu_{nf}=\frac{\mu_{nf}}{\rho_{nf}},$$

$$\frac{\sigma_{nf}}{\sigma_f}=1+\frac{3\left(\frac{\sigma_s}{\sigma_f}-1\right)\varphi}{\left(\frac{\sigma_s}{\sigma_f}+2\right)-\left(\frac{\sigma_s}{\sigma_f}-1\right)\varphi}, \tag{4}$$

where φ is the nanoparticle volume fraction, the subscripts *nf*, *f* and *s* are the thermo-physical properties of the nano-fluids, base fluid and the solid nanoparticles, respectively. The physical properties of the base fluid (drinking water) and different nanoparticles are given in Table 1 (Hatami *et al.* (2014), Oztop and Abu-Nada (2008)). Considering $u_\theta = 0$ for purely radial flow, the velocity parameter can be defined as:

$$f(\theta)=r\,u(r) \tag{5}$$

Introducing the $x = \theta / \alpha$ as the dimensionless degree, the dimensionless form of the velocity parameter can be obtained by dividing that to its maximum value (f_{max}), a dimensional constant which can be related to the flow rate per unit length, as:

$$F(x)=\frac{f(\theta)}{f_{max}} \tag{6}$$

Eliminating P between Eqns. (2) and (3), we obtain

the following problem:

Table 1 Thermo-physical properties of the base fluid and different nanoparticles

Physical properties	Fluid phase (Drinking water)	*CuO*	*Cu*	*Ag*
$\rho\,(kg\,m^{-3})$	997.1	6320	8933	10500
$\sigma\,(S\,m^{-1})$	0.05	4.93×10^{7}	5.96×10^{7}	6.28×10^{7}

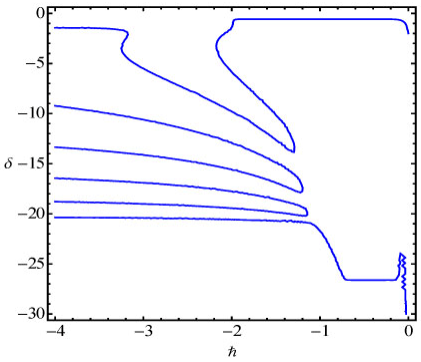

Fig. 2. Prescribed parameter δ via convergence controller parameter $\hbar$ in according to eq. (20) with M = 25 when α = - 1, Re = 10, φ = 0.025 and Mn = 1.

$$F'''(x)+2\alpha\,Re\left(1-\varphi+\frac{\rho_s}{\rho_f}\varphi\right)(1-\varphi)^{2.5}F(x)F'(x)+\left(4-(1-\varphi)^{2.5}\left(1+\frac{3\left(\frac{\sigma_s}{\sigma_f}-1\right)\varphi}{\left(\frac{\sigma_s}{\sigma_f}+2\right)-\left(\frac{\sigma_s}{\sigma_f}-1\right)\varphi}\right)Mn\right)\times\alpha^2F'(x)=0, \tag{7}$$

where $Mn=\sigma_f B_0^2/\mu_f$ is the magnetic parameter and the Reynolds number is:

$$Re=\frac{f_{max}\alpha}{\nu_f}=\frac{U_{max}r\,\alpha}{\nu_f}\quad\begin{pmatrix}divergent\ channel & \alpha>0, & f_{max}>0\\ convergent\ channel & \alpha<0, & f_{max}<0\end{pmatrix} \tag{8}$$

The reduced form of boundary conditions becomes:

$$F(0)=1,\qquad F'(0)=0,\qquad F(1)=0, \tag{9}$$

3. PREDICTOR HOMOTOPY ANALYSIS METHOD (PHAM)

In order to gain PHAM solution, the boundary conditions in eq. (9) become as follows:

$$F(0)=1,\qquad F'(0)=0,\qquad F''(0)=\delta, \tag{10}$$

with the additional forcing condition which plays an important role in PHAM:

$$F(1)=0, \tag{11}$$

Now, we use PHAM for the Eqns. (7) and (10) with prescribed parameter δ. According to the initial conditions:

$$F_0(x,\delta)=1+(\delta/2)\,x^2, \tag{12}$$

In this paper, the auxiliary function has been chosen to be $\mathcal{H}(x)=1$ and the linear operator is as follows:

$$\mathcal{L}_F\left[F(x,\delta;\,q)\right]=\frac{\partial^3F(x,\delta;\,q)}{\partial x^3}, \tag{13}$$

with the properties:

$$\mathcal{L}_F(c_1+c_2\,x+c_3\,x^2)=0, \tag{14}$$

Therefore, after three subsequent integrations, the M^{th} order deformation equation of PHAM yields for $M\geq1$.

$$F_m(x,\delta)=\chi_m\,F_{m-1}(x,\delta)+\hbar\int_0^{\eta}\int_0^{\beta_1}\int_0^{\beta_2}R_m\left(\vec{F}_{m-1},\tau,\delta\right)d\tau\,d\beta_2\,d\beta_1+c_1+c_2\,x+c_3\,x^2, \tag{15}$$

where

$$F'''_{m-1}(\tau,\delta)+2\alpha\,Re\left(1-\varphi+\frac{\rho_s}{\rho_f}\varphi\right)(1-\varphi)^{2.5}\times\sum_{j=0}^{m-1}\left(F_j(\tau,\delta)F''_{m-1-j}(\tau,\delta)\right)+\left(4-(1-\varphi)^{2.5}\left(1+\frac{3\left(\frac{\sigma_s}{\sigma_f}-1\right)\varphi}{\left(\frac{\sigma_s}{\sigma_f}+2\right)-\left(\frac{\sigma_s}{\sigma_f}-1\right)\varphi}\right)Mn\right)\times\alpha^2F'_{m-1}(\tau,\delta)=0, \tag{16}$$

and integration constants c_1, c_2 and c_3 are obtained by the conditions

$$F_m(0,\delta)=F'_m(0,\delta)=F''_m(0,\delta)=0, \tag{17}$$

Using eq.(15), we obtain the functions $F_m(x,\delta)$ for m = 1, 2, 3, … successfully. Finally, we can obtain M^{th} order approximate solution:

$$F_M(x,\delta,\hbar)=\sum_{m=0}^{M}F_m(x,\delta), \tag{18}$$

And the additional forcing condition (11) takes the form of:

$$F_M(1,\delta,\hbar)\approx0, \tag{19}$$

Now, for example, we consider the convergent channel cases, α = -1, in figure 2. Due to the eq

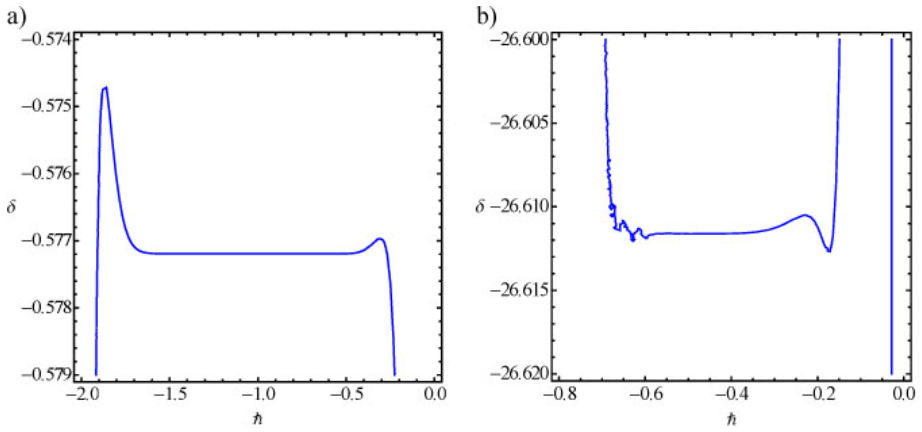

Fig. 3. Prescribed parameter δ via convergence controller parameter $\hbar$ in according to eq. (20) with M = 25 when α = - 1, Re = 10, φ = 0.025 and Mn = 1 (Magnification of Fig. 2).

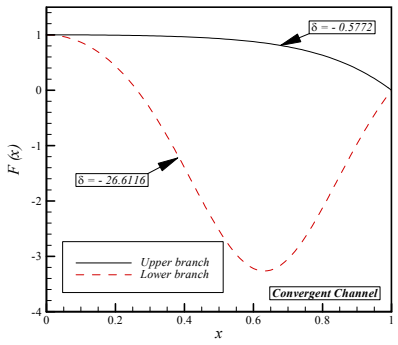

Fig. 4. Dual velocity profile when Re = 10, φ = 0.025 and Mn = 1.

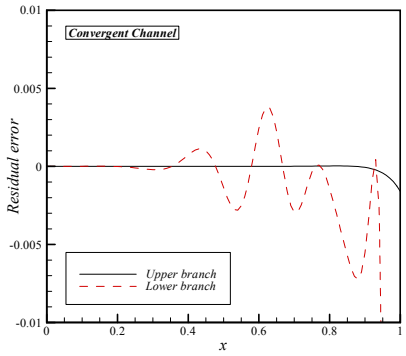

Fig. 5. The residual error for M = 25 when Re = 10, φ = 0.025 and Mn = 1.

(19) in this figure, δ (prescribed parameter) as a function of convergence parameter $\hbar$, has been figured. In order to obtain the values of δ and $\hbar$ with high accuracy, the magnified forms of prescribed parameter as a function of convergence parameter are plotted in figure 3. Two δ-lands can be determined in this figure, namely δ = -0.5722 in the range [-1.6, -0.4] of $\hbar$ and δ = -26.612 in the range [-0.6, -0.3] of $\hbar$. The approximate PHAM solutions of velocity profile correspond to δ = -0.5722 and δ = -26.612, given by (19), are displayed in figure 4. In order to survey the accuracy of these dual approximate solutions, the residual errors of the 25th order of PHAM solutions are illustrated in figure 5. In addition, we compare some of our results with the numerical results obtained by the shooting method coupled with a Runge-Kutta integration method in table 2 to highlight the validity of the applied method for the convergent and divergent channel cases. A very excellent agreement can be observed between them. It should be mentioned that we present two branches of solution via PHAM in table 2, the first line refers to upper branch and the second line refers to lower branch solution.

4. PHAM CALCULATION OF THE TWO BRANCHES OF SOLUTION

In this problem, the multiplicity of solutions (dual solutions) of the eqns. (7) and (9) or equivalently (10), for the convergent channel cases, α = -1, in the parameter plane ($\hbar$, δ), have been identified, we may turn to calculate them explicitly to any desired order M of PHAM-approximation according to eq. (18). We mention that both the upper and lower branches of solutions are calculated at the same time only by eq. (19) with different δ and $\hbar$ which are specified from Fig. 3, δ = -0.5722 and δ = -26.612, respectively for the first and second branches of solutions. As one of the most important advantages of PHAM, there is no need to employ more than one initial approximation guess, one auxiliary linear operator, and one auxiliary function that is in a sharp contrast to all approximation methods which are applied to converge to one solution.

5. RESULTS AND DISCUSSION

The nonlinear ordinary differential equation (7) subject to the boundary conditions (9) is solved analytically via a definitely new analytical technique, PHAM, for some values of the nanoparticle volume fraction parameter (φ), Reynolds number (Re), magnetic parameter (Mn), and angle of the channel (α). We considered three types of nanoparticles, namely, Copper oxide (CuO), Copper (Cu) and Silver (Ag) with water as the base fluid. We remark that the copper

nanoparticle is used in all of the cases in this section

Table 2 Comparison between the $F(x)$ results of PHAM method and the numerical method when Re = Mn = 10 and φ = 0.025

x	α = -1		α = + 1	
	PHAM	Numerical	PHAM	Numerical
0.0	1.000000 1.000000	1.000000	-1.000000	1.000000
0.1	0.998398 0.850663	0.998398	-0.976068	0.976068
0.2	0.993124 0.364276	0.993124	-0.908021	0.908021
0.3	0.982638 -0.546189	0.982638	-0.805855	0.805854
0.4	0.963902 -1.894830	0.963902	-0.682733	0.682732
0.5	0.931554 -3.375230	0.931555	-0.551548	0.551547
0.6	0.876548 -4.249970	0.876549	-0.422423	0.422422
0.7	0.784103 -3.907250	0.784103	-0.301639	0.301638
0.8	0.631079 -2.601420	0.631079	-0.191723	0.191722
0.9	0.383820 -1.124490	0.383820	-0.0921301	0.0921285
1.0	0.000000 0.000000	0.000000	-0.000000	0.000000

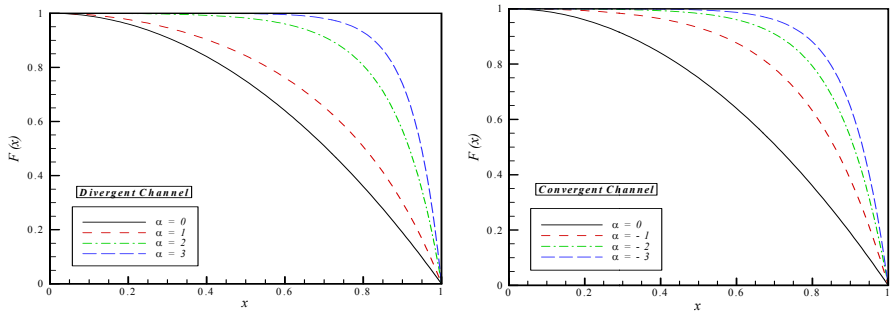

a b

Fig. 6. Effect of the angle between two plates on the velocity profile when Re = Mn = 10 and φ = 0.025.

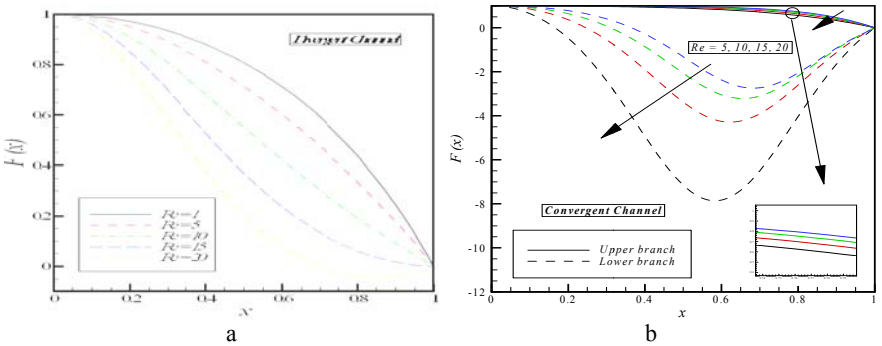

a b

Fig. 7. Effect of the Reynolds number on the velocity profile when φ = 0.025 and Mn = 10.

except for those figures which focus on the influences of the types of applied nanoparticles on the velocity component profiles. For the present investigation, we considered the values of the volume fraction parameter φ vary from 0 (regular Newtonian fluid) to 0.1.

Effect of the angle between two plates on the velocity profile is displayed in figure 6. Note that the rigid walls are considered divergent channel when $\alpha > 0$ and convergent when $\alpha < 0$. As α increases, the divergent channel cases, the effect of walls on the fluid flow decreases, when we move away from them which lead to an increase of velocity; however there is a reverse behavior in velocity profile for the convergent channel cases.

Fig. 7 presents the effect of Reynolds number for the divergent and convergent channel with slope 1°, respectively. In the divergent channel cases, the results show that increasing in Reynolds number make a decrease in velocity profile. Furthermore, the flow moves reversely and a region of back flow near the wall is observed for the higher Reynolds number ($Re \geq 20$). In addition, for convergent channel, results are inversed and by increasing the Reynolds number, velocity profiles are enhanced. As the results illustrate, the dual solutions exist in the convergent channel cases.

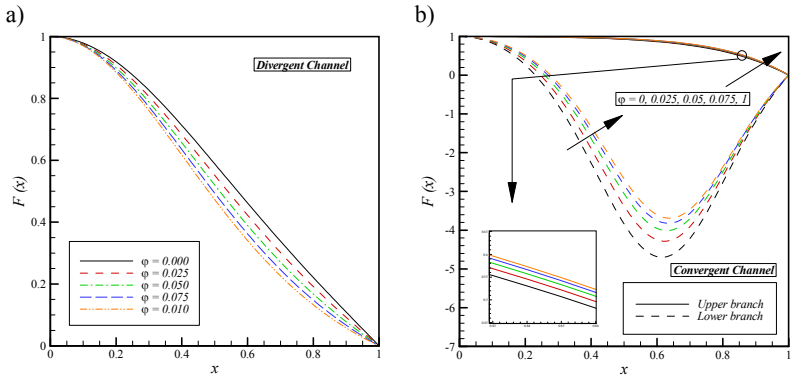

Fig. 8. Effect of the nanoparticle volume fraction parameter on the velocity profile when *Re* = *Mn* = 10.

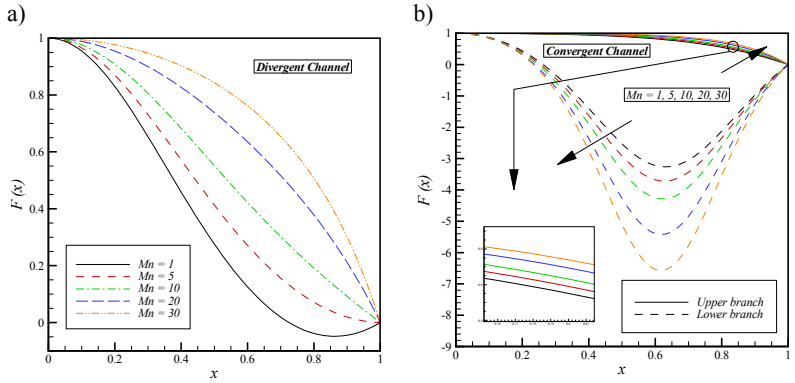

Fig. 9. Effect of the magnetic parameter on the velocity profile when *Re* = 10 and *φ* = 0.025.

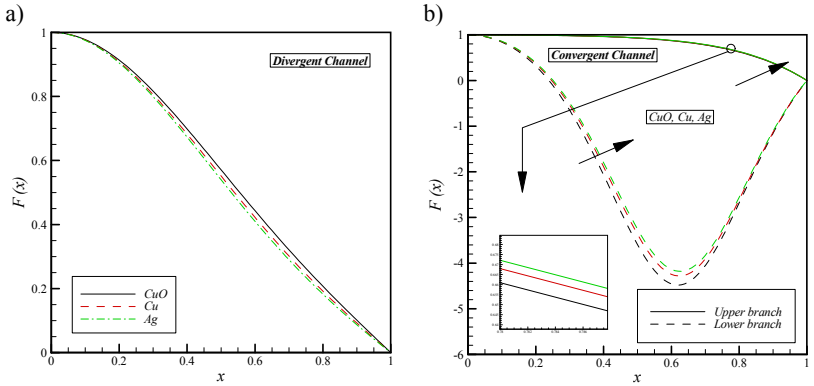

Fig. 10. Effect of different nanoparticle types' on the velocity profile when *Re* = *Mn* = 10 and *φ* = 0.025.

Fig. 8 depicts the effect of nanoparticle volume fraction parameter on the velocity profile for a divergent and convergent channel with 1° slope. It can be seen that increasing nanoparticle volume fraction parameter in divergent channel lead to decrease velocity profile. The results are inversed for the convergent channel cases.

The effect of magnetic parameter for a divergent and convergent channel is illustrated in figure 9. The velocity profiles show that the rate of transport is considerably reduced with increase of M. This clearly display that the transverse magnetic field opposes the transport phenomena. Because of this fact that the variation of M leads to the variation of the Lorentz force due to magnetic field and the Lorentz force produces more resistance to transport phenomena. Increasing in the magnetic parameter makes an increase in velocity profile. In addition, the flow reversal disappears by the increasing of M for the divergent channel cases.

Finally, the effect of different nanoparticle types on the velocity profile is displayed in figure 10. It is obvious that selecting copper oxide (*CuO*) as a nanoparticle leads to maximum values in the velocity profile, but this treatment of nano-fluids structure is completely vice versa for convergent channels.

6. CONCLUSION

In this study, Predictor Homotopy Analysis Method (PHAM) as a new analytical technique was applied to solve the problem of MHD Jeffery–Hamel nano-fluid flow in non-parallel walls for the divergent and convergent channels. This applied method is very powerful especially for those boundary value problems which admit multiple solutions and also is capable to calculate all branches of the solutions simultaneously. For the current problem, it was found that the dual solutions existed for the convergent channel cases (α = -1). The results of current study were compared with the numerical solution obtained using the shooting method, coupled with a Runge-Kutta scheme. We found that the analytical solution matches the numerical solution quite well. In continued, the effects of the nanoparticle volume fraction parameter, Reynolds number, magnetic parameter, and angle of the channel as well as different types of nanoparticles on the flow were discussed in details.

REFERENCES

Abbas, Z., Y. Wang, T. Hayat and M. Oberlack (2010). Mixed convection in the stagnation-point flow of a Maxwell fluid towards a vertical stretching surface. *Nonlinear Analysis: Real World Applications* 11(4), 3218-3228.

Abbasbandy, S. and E. Shivanian (2014). Chapter 2: Predictor Homotopy Analysis Method (PHAM). *Advances in the Homotopy Analysis Method*. 35-83.

Abbasbandy, S. and E. Shivanian (2011). Predictor homotopy analysis method and its application to some nonlinear problems. *Communications in Nonlinear Science and Numerical Simulation* 16, 2456-2468.

Bachok, N., A. Ishak and I. Pop (2010). Boundary-layer flow of nanofluids over a moving surface in a flowing fluid. *International Journal of Thermal Sciences* 49(9), 1663-1668.

Brinkman, H. C. (1952). The viscosity of concentrated suspensions and solutions. *Journal of Chemical Physics* 20(4), 571.

Choi, S. U. S. and J. A. Eastman (1995). Enhancing thermal conductivity of fluids with nanoparticles. *Materials Science* 231, 99-105.

Eastman, J. A., U. S. Choi, S. Li, G. Soyez, L. J. Thompson and R. J. DiMelfi (1999). Novel Thermal Properties of Nanostructured Materials. *Materials Science Forum* 312 - 314, 629-634.

Hatami, M. and D. D. Ganji (2014). MHD nanofluid flow analysis in divergent and convergent channels using WRMs and numerical method. *International Journal of Numerical Methods for Heat & Fluid Flow* 24(5), 1191-1203.

Hatami, M., M. Sheikholeslami, M. Hosseini and D. D. Ganji (2014). Analytical investigation of MHD nanofluid flow in non-parallel walls. *Journal of Molecular Liquids* 194(0), 251-259.

Hayat, T., Z. Abbas and M. Sajid (2009). MHD stagnation-point flow of an upper-convected Maxwell fluid over a stretching surface. *Chaos, Solitons & Fractals* 39(2), 840-848.

Hooper, A., B. R. Duffy and H. K. Moffatt (1982). Flow of fluid of non-uniform viscosity in converging and diverging channels. *Journal of Fluid Mechanics* 117, 283-304.

JIANG Bing-li and L. Yin-ping (2013). Predictor homotopy analysis method and its application to two nonlinear systems. Journal of East China Normal University (3), 131-139.

Kato, H. and H. Shibanuma (1980). Diverging Converging Flows of Dilute Polymer Solutions : 1st Report, Pressure Distribution and Velocity Profile. *Japan Society of Mechanical Engineers* 23(181), 1140-1147.

Liao, S. J. (2004a). *Beyond perturbation: introduction to the homotopy analysis method*. Chapman & Hall/CRC

Liao, S. J. (2004b). On the homotopy analysis method for nonlinear problems. *Applied Mathematics and Computation* 147(2), 499-513.

Mahian, O., S. Mahmud and S. Z. Heris (2012). Analysis of entropy generation ween co-rotating cylinders using nanofluids. *Energy* 44(1), 438-446.

Moghimi, S. M., G. Domairry, S. Soleimani, E. Ghasemi and H. Bararnia (2011). Application of homotopy analysis method to solve MHD Jeffery–Hamel flows in non-parallel walls. *Advances in Engineering Software* 42(3), 108-113.

Moradi, A., A. Alsaedi and T. Hayat (2013). Investigation of Nanoparticles Effect on the Jeffery–Hamel Flow. *Arabian Journal for Science and Engineering* 38(10), 2845-2853.

Oztop, H. and E. Abu-Nada (2008). Numerical study of natural convection in partially heated rectangular enclosures filled with nanofluids.

International Journal of Heat and Fluid Flow 29(5), 1326-1336.

Rashidi, M. M., S. Abelman and N. Freidoonimehr (2013a). Entropy generation in steady MHD flow due to a rotating porous disk in a nanofluid. *International Journal of Heat and Mass Transfer* 62(0), 515-525.

Rashidi, M. M., M. Ali, N. Freidoonimehr and F. Nazari (2013b). Parametric analysis and optimization of entropy generation in unsteady MHD flow over a stretching rotating disk using artificial neural network and particle swarm optimization algorithm. *Energy* 55(0), 497-510.

Rashidi, M. M., M. Ali, N. Freidoonimehr, B. Rostami and M. A. Hossain (2014c). Mixed Convective Heat Transfer for MHD Viscoelastic Fluid Flow over a Porous Wedge with Thermal Radiation. *Advances in Mechanical Engineering* 2014, 10.

Rashidi, M. M., N. Freidoonimehr, A. Hosseini, O. A. Bég and T. K. Hung (2014a). Homotopy simulation of nanofluid dynamics from a non-linearly stretching isothermal permeable sheet with transpiration. *Meccanica* 49(2), 469-482.

Rashidi, M. M., B. Rostami, N. Freidoonimehr and S. Abbasbandy (2014b). Free convective heat and mass transfer for MHD fluid flow over a permeable vertical stretching sheet in the presence of the radiation and buoyancy effects. *Ain Shams Engineering Journal*

Sadeghy, K., N. Khabazi and S. Taghavi (2007). Magnetohydrodynamic (MHD) flows of viscoelastic fluids in converging/diverging channels. *International Journal of Engineering Science* 45(11), 923-938.

Sheikholeslami, M. and D. D. Ganji (2014a). Three dimensional heat and mass transfer in a rotating system using nanofluid. *Powder Technology* 253(0), 789-796.

Sheikholeslami, M. and D. D. Ganji (2014b). Numerical investigation for two phase modeling of nanofluid in a rotating system with permeable sheet. *Journal of Molecular Liquids* 194(0), 13-19.

Sheikholeslami, M., D. D. Ganji, H. R. Ashorynejad and H. B. Rokni (2012). Analytical investigation of Jeffery-Hamel flow with high magnetic field and nanoparticle by Adomian decomposition method. *Applied Mathematics and Mechanics* 33(1), 25-36.

Shivanian, E. and S. Abbasbandy (2014). Predictor homotopy analysis method: Two points second order boundary value problems. *Nonlinear Analysis: Real World Applications* 15, 89-99.

Vosoughi, H., E. Shivanian and S. Abbasbandy (2012). Unique and multiple PHAM series solutions of a class of nonlinear reactive transport model. *Numerical Algorithms* 61, 515-524.

Xuan, Y. and Q. Li (2003). Investigation on Convective Heat Transfer and Flow Features of Nanofluids. *Journal of Heat Transfer* 125(1), 151-155.